4th Micro and Nano Flows Conference
UCL, London, UK, 7-10 September 2014

Dynamic unbinding transitions and deposition patterns in dragged meniscus problems

Mariano GALVAGNO[1,*], Dmitri TSELUIKO [1], Uwe THIELE [1,2]

* Corresponding author: Tel.: +44(0)1509228206; Fax: +44(0)1509223969; Email: mgalvagno@gmail.com
1: Department of Mathematical Sciences, Loughborough University, Loughborough, Leicestershire, LE11 3TU, UK
2: Institut für Theoretische Physik, Westfälische Wilhelms-Universität Münster, Wilhelm Klemm Str. 9, D-48149 Münster, Germany

Abstract We sketch main results of our recent work on the transfer of a thin liquid film onto a flat plate that is extracted from a bath of pure non-volatile liquid. Employing a long-wave hydrodynamic model, that incorporates wettability via a Derjaguin (disjoining) pressure, we analyse steady-state meniscus profiles as the plate velocity is changed. We identify four qualitatively different dynamic transitions between microscopic and macroscopic coatings that are out-of-equilibrium equivalents of equilibrium unbinding transitions. The conclusion briefly discusses how the gradient dynamics formulation of the problem allows one to systematically extend the employed one-component model into thermodynamically consistent two-component models as used to describe, e.g., the formation of line patterns during the Langmuir-Blodgett transfer of a surfactant layer.

1. Introduction

The study of the transfer of a film or patterned deposit onto a flat plate that is extracted from a bath of pure liquid or solution/suspension is of significant interest due to numerous industrial applications. The understanding of the various interfacial effects on small scales becomes increasingly important because of the intense drive towards a further miniaturisation of fluidic systems.

On the one hand, it is a classical hydrodynamic problem to study how droplets slide down an incline [1, 2, 3, 4], how moving contact lines (where solid, gas and liquid meet) develop sawtooth shapes at high speeds [4, 5, 6], or how the free surface of a bath is deformed when a plate is drawn out, as sketched in Fig. 1(a). On the other hand, the equilibrium behaviour of films, drops and menisci is studied by means of statistical physics using energy functionals, and various phase transitions, e.g., wetting and emptying transitions have been analysed in the literature, see [7].

Here, we focus on the case of a pure non-volatile liquid employing a long-wave hydrodynamic model in gradient dynamics formulation, that incorporates wettability via a Derjaguin (disjoining) pressure. We use this model to investigate the nonequilibrium transitions between meniscus and film solutions and identify four qualitatively different dynamic unbinding transitions – continuous and discontinuous dynamic wetting and emptying transitions.

2. Drawn film flow

We consider a flat plate that forms a constant angle with the horizontal direction and that is being withdrawn from a pool of liquid at a constant speed. A schematic representation of the system is shown in Fig. 1. A Cartesian coordinate system (x, z) is introduced where the x-axis points along the plate in downwards direction and the z-axis is perpendicular to the plate and points into the liquid. We assume that the system is two-dimensional, i.e., there are no variations in the transverse direction. The position of the free surface is then given by

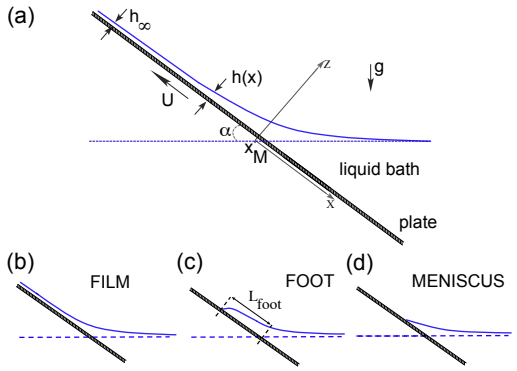

Figure 1: Sketches of (a) the considered two-dimensional geometry and (b-d) of the qualitatively different steady shapes $h(x)$ of the free liquid surface as found in experiments: (b) *Landau-Levich film*, (c) *foot* or *extended meniscus*, and (d) *simple meniscus*. In panel (c) we indicate the typical foot length $L_{\rm foot}$ (see main text for details).

$z = h(x,t)$, where t denotes time. The scales employed in the non-dimensionalisation are $\ell = \sqrt{3/5}h_{\rm eq}/\theta_{\rm eq}$, $h_{\rm eq}$ and $\tau = (3\eta h_{\rm eq})/(25\gamma\theta_{\rm eq}^4)$ for the x-coordinate, film height and time, respectively, where γ is the surface tension, η is the viscosity of the liquid and $h_{\rm eq}$ and $\theta_{\rm eq}$ are the equilibrium precursor height and contact angle, respectively.

We formulate the non-dimensional evolution equation for a conserved film thickness of a simple non-volatile liquid using a gradient dynamic model based on an interface Hamiltonian $F[h]$ (aka free energy) that additionally includes potential energy, i.e.,

$$\partial_t h = \partial_x \left[Q(h)\partial_x \frac{\delta F[h]}{\delta h} \right] + U\partial_x h. \qquad (1)$$

For this particular problem, $Q(h) = h^3/3$ is the mobility and

$$F[h] \approx \int_A \left[\frac{1}{2}|\partial_x h|^2 + f(h) + G\left(\frac{h^2}{2} - \alpha h x\right) \right] {\rm d}A, \qquad (2)$$

where $f(h)$ is the wetting or adhesion energy and the final terms represent the potential energy in long-wave scaling. Here U, G and α are the dimensionless parameters that represent plate velocity (Capillary number), gravity (Bond number), and the scaled $O(1)$ inclination angle of the plate, respectively (see note [8]). Due to the boundary conditions on the bath side (discussed below) the model is not invariant with respect to translations in x, i.e., the existence of the bath selects the physical laboratory system as a particular frame of reference. Therefore the advection term $U\partial_x h$ can not be removed by a Galilean transformation.

Note that this gradient dynamics model corresponds exactly to the hydrodynamic long-wave or lubrication equation

$$\begin{aligned} \partial_t h &= -\partial_x \left\{ Q(h)\partial_x [\partial_x^2 h + \Pi(h) - Gh] \right\} \\ &\quad -\partial_x Q(h) G\alpha + U\partial_x h, \end{aligned} \qquad (3)$$

that can be derived from the Navier-Stokes equations and the corresponding boundary conditions under the assumptions that the physical plate inclination angle and equilibrium contact angle are small.

The partial wettability of the liquid on the chosen substrate is described via the Derjaguin (or disjoining) pressure [9]

$$\Pi = -\frac{1}{h^3}\left(1 - \frac{1}{h^3}\right), \qquad (4)$$

derived in Ref. [10] from a modified Lennard-Jones potential with hard-core repulsion. The disjoining pressure is related to a wetting or adhesion energy $f(h)$ via $\Pi = -df/dh$, cf. [8].

To calculate steady film and meniscus profiles one sets $\partial_t h = 0$, then integrates Eq. (3) once and solves the resulting three-dimensional dynamical system in $(h, \partial_x h, \partial_{xx} h)$ with appropriate boundary conditions: (i) far from the bath one imposes that the film profile approaches a flat film of unknown height h_∞ while (ii) the approach towards the bath for $x \to \infty$ is described by an asymptotic series rigorously derived via a centre manifold reduction [11]. To do so, we introduce a change of variables $y_1 = 1/h$, $y_2 = h'$ and $y_3 = h''$ following a proposal of Ref. [12], and convert the steady-state equation into the

three-dimensional dynamical system

$$y_1' = -y_1^2 y_2, \quad (5)$$
$$y_2' = y_3, \quad (6)$$
$$y_3' = (6y_1^7 - 3y_1^4)y_2 + Gy_2 + Uy_1^2 - C_0 y_1^3 - G\alpha. \quad (7)$$

This is used to obtain a new fixed point corresponding to the bath, namely the point $y_b = (0, \alpha, 0)$, beside other fixed points, two of which, $y_f = (1/h_f, 0, 0)$ and $y_p = (1/h_p, 0, 0)$, correspond to the foot and the precursor film, respectively. The centre manifold analysis then yields the asymptotic sequence [11]

$$h \sim \alpha x + D_1 x^{-1} + D_2 x^{-2} + D_3 x^{-3} + \cdots, \quad (8)$$

where

$$D_1 = \frac{U}{\alpha^2 G}, \qquad D_2 = -\frac{C_0}{2\alpha^3 G},$$
$$D_3 = -\frac{1}{3}\left(\frac{2U^2}{\alpha^5 G} + \frac{3}{\alpha^3 G} - \frac{6U}{\alpha^2 G^2}\right), \ldots. \quad (9)$$

The steady profiles and bifurcation diagrams are numerically obtained employing pseudo-arclength continuation [13]. The main solution measure is the dynamic excess volume $\Delta V = V - V_0$ with $V = \int (h(x) - h_\infty) dx$, where V_0 is V at $U = 0$.

2.1 Results

In the following we sketch main results presented in Ref. [14] and further analysed in Ref. [11]. Ref. [14] analyses the changes that steady menisci undergo with increasing plate speed U that can be presented in the form of bifurcation diagrams where, e.g., the solution measure ΔV is given in dependence of U. Depending on the plate inclination angle α four qualitatively different bifurcation diagrams are found as illustrated in Fig. 2 together with steady height profiles for selected values of U. Each of these cases is related to a distinguished nonequilibrium unbinding transition.

(a) At small inclination angles α, e.g., $\alpha = 0.1$, the volume ΔV monotonically increases: first slowly, then faster until it diverges at about

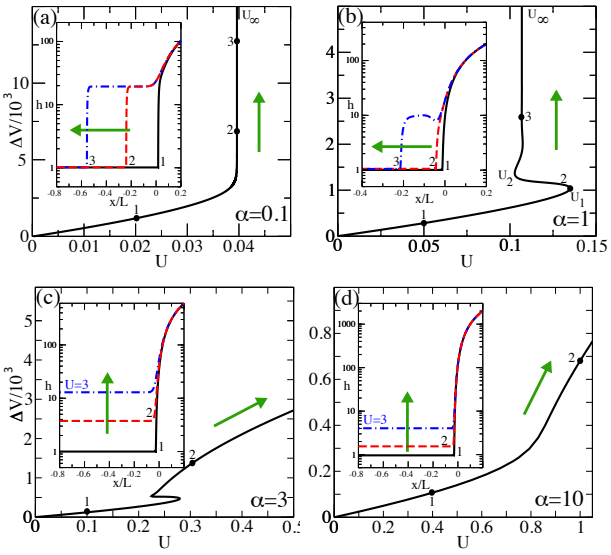

Figure 2: Four qualitatively different bifurcation curves at different plate inclination angles in increasing order: (a) $\alpha = 0.1$, (b) $\alpha = 1$, (c) $\alpha = 3$, and (d) $\alpha = 10$. The main panels shown the excess volume ΔV (scaled for convenience by 10^3) in dependence on the plate velocity U, the insets give Log-normal representations of steady film profiles as indicated by corresponding labels. The domain size is $L = 1000$. Corresponds to amended Fig. 2 of [14].

$U_\infty \approx 0.04$, see Fig. 2(a). The corresponding simple meniscus profiles first deform only slightly due to viscous bending before a distinguished foot-like protrusion of a height $h_f \approx 10$ develops whose length L_{foot}[1] diverges $\propto \ln[(U_\infty - U)/U_\infty]^{-1}$. This corresponds to a continuous dynamic emptying transition, that may be seen as a non-equilibrium analogue of the equilibrium transition analysed in Ref. [7]. One could say that at U_∞ the tip of the foot unbinds from the meniscus and ultimately the bath is emptied. For $U > U_\infty$ the foot advances with a constant velocity $V_F \approx (U - U_\infty)$, what in a finite system will result in a transition to a Landau-Levich film. Far away from the bath such a Landau-Levich coating layer has a thickness $h_\infty \propto U^{2/3}$ [15]. The transition looks similar to the one presented for a larger α in Fig. 3(b).

[1] We define the measure for the foot length $L_{foot} \propto \Delta V/(h_f - h_\infty)$, where h_f is the foot height and h_∞ the coating film height.

(b) Above a first critical angle $\alpha = \alpha_1 \approx 0.103$, the transition changes its character and becomes a discontinuous dynamic emptying transition without an equilibrium analogue. As shown in Fig. 2(b), ΔV increases first monotonically with U until the first saddle-node bifurcation occurs at U_1 where the curve folds back. Following the curve further, one finds that it folds again at U_2. The folding back and forth infinitely continues at loci that exponentially approach U_∞ from both sides and that separate linearly stable and unstable foot solutions. It can be shown that this exponential (or collapsed) snaking [16] results from the existence of a heteroclinic chain connecting the fixed points of the system (5)–(7) corresponding to the precursor film, the foot and the bath height under the condition that the fixed point corresponding to the foot is a saddle-focus with two-dimensional unstable manifold. This results in foot length with $[(U_\infty - U)/U_\infty]^{-1} \propto \exp(\mathrm{Re}[\nu]L_{\mathrm{foot}})\sin(\mathrm{Im}[\nu]L_{\mathrm{foot}})$ where ν is a linear eigenvalue whose real and imaginary part determine the exponential approach and the period of the snaking, respectively [11]. Note that for $U > U_\infty$ one can always find a critical foot length beyond which the foot advances. In contrast, for $U < U_\infty$ there is always a critical length above which a foot recedes. The receding and advancing case are illustrated for $\alpha = 0.5$ in the space-time plots of Figs. 3(a) and 3 (b), respectively. The advancing and receding foot-like structures can be characterised by the constant velocity V_{F} of their tip. It is found that V_{F} is always equal to the velocity difference $U - U_\infty^\alpha$ where U_∞^α depends on the plate inclination α, that is a direct consequence of the Galilean invariance of the system in the absence of the bath as the moving tip can be seen as being detached from the bath. It should also be noted that U_∞^α corresponds to the velocity a large flat (pancake-like) drop selects that freely slides down a resting plate inclined at an angle α (see [14] and cf. [2]).

(c) At a second critical angle $\alpha = \alpha_2 \approx 2.42$, the bifurcation diagram dramatically changes. Above α_2 the family of steady meniscii that one follows when starting at the meniscus solution at $U = 0$ does not anymore diverge at a limiting velocity U_∞. No foot of increasing length emerges that unbinds from the meniscus. Instead one finds a hysteretic transition [in Fig. 2(c) between $U = 0.1$ and 0.3] towards a coating layer whose thickness homogeneously increases with increasing U, i.e., the layer surface unbinds from the substrate in a discontinuous dynamic wetting transition.

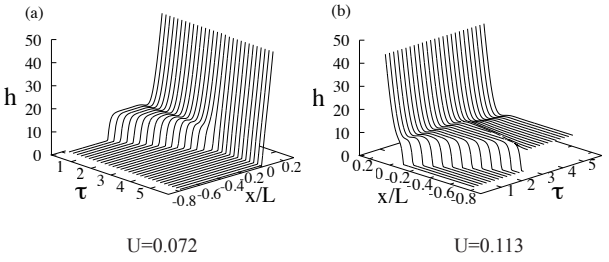

U=0.072 U=0.113

Figure 3: Panels (a) and (b) give for $\alpha = 0.5$ space-time plots representing the time evolution of a receding and an advancing foot, respectively, at values of U as indicated indicated in the figures. The evolution in (a) converges to a steady simple meniscus (receding), while in (b) the foot advances with constant speed until its tip reaches the domain boundary, then at $\tau \approx 4$ the foot transforms into a Landau-Levich film. Corresponds to inset of Fig. 3 of [14].

(d) With increasing angle α the hysteresis of the discontinuous transition becomes smaller until at a third critical angle $\alpha = \alpha_3 \approx 5.92$ the two saddle-node bifurcations annihilate in a hysteresis bifurcation. For all $\alpha > \alpha_3$ one finds a continuous dynamic wetting transition.

In cases (c) and (d) the coating layer thickness at large U follows the power law $h_\infty \propto U^{2/3}$. This allows one to identify these unbinding film states as Landau-Levich films [15]. The critical velocity where the transition between the microscopic and macroscopic layer occurs, scales as $\alpha^{3/2}$.

3. Conclusions

We have sketched some main results of our recent work [11, 14] on the transfer of a thin liquid film onto a flat plate. In particular, we have used a long-wave mesoscopic hydrody-

namic description of a coating problem (inclined plate drawn from a bath) incorporating wettability via a Derjaguin pressure to identify and analyse several qualitatively different transitions with increasing plate speed. We have distinguished four ranges of inclination angles where different dynamic unbinding transitions occur, namely *continuous* and *discontinuous dynamic emptying transitions* and *discontinuous* and *continuous dynamic wetting transitions*. These dynamic transitions are out-of-equilibrium equivalents of known equilibrium emptying and wetting transitions and have important features without equilibrium equivalent.

We refer the reader to Ref. [14] for more information on the various non-equilibrium unbinding transitions, while we recommend Ref. [11] for (i) the centre manifold reduction that allowed us to rigorously derive the asymptotic series that describes the approach towards the bath (including for films drawn by a temperature gradient), and for (ii) the Shilnikov-type analysis that shows the relation of exponential (or collapsed) snaking and the existence of a heteroclinic chain. The latter is complemented by a detailed numerical analysis of the transition between continuous and discontinuous dynamic emptying transitions.

We finally point out that in many practically important cases the transferred liquid is not a simple non-volatile one. Often suspensions or solutions with volatile solvents are used resulting, e.g., in dip coating processes in the production of homogeneous or patterned functional coatings. An example is the Langmuir-Blodgett transfer of a surfactant layer from a bath onto a moving plate as experimentally studied in [17, 18] and modelled with a two-component thin film model in Ref. [19] and a Cahn-Hilliard-type model in [20]. Many other examples of pattern formation at externally driven contact lines are listed in the review on deposition patterns [21], there categorised as deposition in *active geometries*. In such systems film deposition, evaporation and various phase transitions may conspire to produce a variety of patterns as, e.g., regular line patterns. In the case of Langmuir-Blodgett transfer emerging stripe patterns can be related to a first order structural phase transition in the surfactant layer that results from a substrate-mediated condensation effect [17]. However, hydrodynamic long-wave models for suspensions and solutions are often rather restricted concerning the spectrum of physical effects that can be included in a systematic and consistent way. For instance, the models used in [22] to study line deposition do not take effects like solvent-solute interactions or solute-dependent wettability into account. Attempts to add such effects to the long-wave model in an ad-hoc manner have in the past sometimes resulted in inconsistent or even unphysical models.

A systematic way for such extensions of hydrodynamic long-wave models has recently been proposed for non-surface active solutes [23] and insoluble surfactants [24] based on a gradient dynamics form as Eq. (1) above. An extension of Eq. (1) towards two fields (e.g., local film height h and local solute/surfactant amount ψ) for a suspension or solution transferred from a bath onto a moving plate has the form (written in the 2d case)

$$\begin{aligned} \partial_t h &= \partial_x \left[Q_{hh} \partial_x \frac{\delta F}{\delta h} + Q_{h\psi} \partial_x \frac{\delta F}{\delta \psi} \right] + U \partial_x h, \\ \partial_t \psi &= \partial_x \left[Q_{\psi h} \partial_x \frac{\delta F}{\delta h} + Q_{\psi\psi} \partial_x \frac{\delta F}{\delta \psi} \right] + U \partial_x \psi \end{aligned} \tag{10}$$

where

$$\mathbf{Q} = \begin{pmatrix} Q_{hh} & Q_{h\psi} \\ Q_{\psi h} & Q_{\psi\psi} \end{pmatrix} \tag{11}$$

is a symmetric and positive definite mobility matrix and $F[h,\psi]$ is an appropriate free energy functional. For details see [23, 24] and also the conclusion of [21] where limitations and alternative approaches are discussed as well. A volatile solvent can be accounted for by adding a term proportional to $\mu - \delta F/\delta h$, i.e., an evaporation flux, to the first equation of (10); here μ is the chemical potential of the surrounding gas phase. This will be further explored in the future.

Acknowledgements

We acknowledge support by the EU via the FP7 Marie Curie scheme (ITN MULTIFLOW, PITN-GA-2008-214919). The work of DT was partly supported by the EPSRC under grants EP/J001740/1, EP/K041134/1.

References

[1] T. Podgorski, J.-M. Flesselles, and L. Limat. Corners, cusps, and pearls in running drops. Phys. Rev. Lett., 87:036102, 2001.

[2] U. Thiele, K. Neuffer, M. Bestehorn, Y. Pomeau, and M. G. Velarde. Sliding drops on an inclined plane. Colloid Surf. A - Physicochem. Eng. Asp., 206:87–104, 2002.

[3] M. Ben Amar, L. J. Cummings, and Y. Pomeau. Transition of a moving contact line from smooth to angular. Phys. Fluids, 15:2949–2960, 2003.

[4] J. H. Snoeijer and B. Andreotti. Moving contact lines: Scales, regimes, and dynamical transitions. Annu. Rev. Fluid Mech., 45:269–292, 2013.

[5] T. D. Blake and K. J. Ruschak. A maximum speed of wetting. Nature, 282:489–491, 1979.

[6] G. Delon, M. Fermigier, J. H. Snoeijer, and B. Andreotti. Relaxation of a dewetting contact line. part 2. experiments. J. Fluid Mech., 604:55–75, 2008.

[7] A. O. Parry, C. Rascon, E. A. G. Jamie, and D. G. A. L. Aarts. Capillary emptying and short-range wetting. Phys. Rev. Lett., 108:246101, 2012.

[8] The velocity scale, gravity number and the scaled inclination angle are given by $3\tau/\ell$, $G = \rho g h_{\rm eq}^4/A$, and $\alpha = (\ell/h_{\rm eq})\tilde{\alpha} = O(1)$, respectively, where ρ, η and γ are the density, viscosity and surface tension of the liquid, and g is gravitational accelleration. The physical plate inclination angle $\tilde{\alpha}$ is assumed to be small, thereby ensuring uniform validity of the long-wave model in precursor, mensicus and bath region. For the dimensional disjoining pressure $\Pi = -A/h^3 + B/h^6$, with Hamaker constant $A > 0$ and short-range interaction strength $B > 0$, the equilibrium precursor height and contact angle are $h_{\rm eq} = (B/A)^{1/3}$ (i.e., the scaled precursor height is $h_p = 1$) and $\theta_{\rm eq} = \sqrt{3A/5\gamma h_{\rm eq}^2}$ (i.e., the scaled equilibrium contact angle is $\sqrt{3/5}$), respectively. We use $G = 0.001$.

[9] V. M. Starov and M. G. Velarde. Surface forces and wetting phenomena. J. Phys.-Condes. Matter, 21:464121, 2009.

[10] L. M. Pismen. Mesoscopic hydrodynamics of contact line motion. Colloid Surf. A-Physicochem. Eng. Asp., 206:11–30, 2002.

[11] D. Tseluiko, M. Galvagno, and U. Thiele. Collapsed heteroclinic snaking near a heteroclinic chain in dragged meniscus problems. Eur. Phys. J. E, 37:33, 2014.

[12] A. Münch and P.L. Evans. Marangoni-driven liquid films rising out of a meniscus onto a nearly-horizontal substrate. Phys. D (Amsterdam, Neth.), 209(1-4):164 – 177, 2005. Non-linear Dynamics of Thin Films and Fluid Interfaces.

[13] H. A. Dijkstra, F. W. Wubs, A. K. Cliffe, E. Doedel, I. F. Dragomirescu, B. Eckhardt, A. Y. Gelfgat, A. Hazel, V. Lucarini, A. G. Salinger, E. T. Phipps, J. Sanchez-Umbria, H. Schuttelaars, L. S. Tuckerman, and U. Thiele. Numerical bifurcation methods and their application to fluid dynamics: Analysis beyond simulation. Commun. Comput. Phys., 15:1–45, 2014.

[14] M. Galvagno, D. Tseluiko, H. Lopez, and U. Thiele. Continuous and discontinuous dynamic unbinding transitions in drawn film flow. Phys. Rev. Lett., 112:137803, 2014.

[15] L. Landau and B. Levich. Dragging of a liquid by a moving plane. Acta Physicochimica URSS, 17:42, 1942.

[16] Y. P. Ma, J. Burke, and E. Knobloch. Defect-mediated snaking: A new growth mechanism for localized structures. Physica D, 239:1867–1883, 2010.

[17] H. Riegler and K. Spratte. Structural-changes in lipid monolayers during the Langmuir-Blodgett transfer due to substrate monolayer interactions. Thin Solid Films, 210:9–12, 1992.

[18] S. Lenhert, L. Zhang, J. Mueller, H. P. Wiesmann, G. Erker, H. Fuchs, and L. F. Chi. Self-organized complex patterning: Langmuir-Blodgett lithography. Adv. Mater., 16:619–624, 2004.

[19] M. H. Köpf, S. V. Gurevich, R. Friedrich, and L. F. Chi. Pattern formation in monolayer transfer systems with substrate-mediated condensation. Langmuir, 26:10444–10447, 2010.

[20] M. H. Köpf, S. V. Gurevich, R. Friedrich, and U. Thiele. Substrate-mediated pattern formation in monolayer transfer: a reduced model. New J. Phys., 14:023016, 2012.

[21] U. Thiele. Patterned deposition at moving contact line. Adv. Colloid Interface Sci., 206:399–413, 2014.

[22] L. Frastia, A. J. Archer, and U. Thiele. Modelling the formation of structured deposits at receding contact lines of evaporating solutions and suspensions. Soft Matter, 8:11363–11386, 2012.

[23] U. Thiele, D. V. Todorova, and H. Lopez. Gradient dynamics description for films of mixtures and suspensions: Dewetting triggered by coupled film height and concentration fluctuations. Phys. Rev. Lett., 111:117801, 2013.

[24] U. Thiele, A. J. Archer, and M. Plapp. Thermodynamically consistent description of the hydrodynamics of free surfaces covered by insoluble surfactants of high concentration. Phys. Fluids, 24:102107, 2012.